LUND UNIVERSITY
Faculty of Science

A Planar Laser-induced Fluorescence Study of NO + CO oxidation at Pd(100)

Hanna Sjö

Thesis submitted for the degree of Bachelor of Science
Project duration: 2 months

Supervised by Johan Zetterberg and Sebastian Pfaff

Department of Physics
Division of Combustion Physics
May 2020

Abstract

Catalysis is an essential tool in industry, and the developments in catalysis research during the last decades have led to higher efficiency in many important processes. CO oxidation is a common reaction to use in catalysis research both due to its applications in industry but also since it is a simple reaction where the knowledge gained about its reaction mechanism can be applied to important but more complicated reactions.

There is an active debate within the catalysis field regarding the phase where late transition metals, such as Pd, are active. Thin layer surface oxides are by some considered inactive and by others equally or more active than the metallic surface. Lorentzi et al. performed a theoretical study of simultaneous CO and NO oxidation. The predictions of the study were that the NO under some gas conditions prevents the formation of surface oxide, and thus, under the assumption that the oxide is inactive, improves the activity both through this removal and by other synergistic effects.

This thesis tries to experimentally determine the effects of NO in CO oxidation at a single crystal Pd(100) surface. This is further connected to the activity of the sample. Surface optical reflectance and planar laser-induced fluorescence are used to get comparable measurements of surface reflection intensity and gas composition in the vicinity of the surface for reactions with and without small amounts of NO for two different O_2:CO ratios.

The result was that the surface optical reflectance measurements were approximately constant during the entire reaction process when NO was present in the gas mixture, implying the lack of oxide formation. However, the CO oxidation activity, shown by the planar laser-induced fluorescence measurements, was limited by the presence of NO. The activity had a more significant decrease at higher O_2:CO ratios. The limitation can be concluded to be caused by limitations in surface access for the CO caused by NO at the surface.

Contents

1 Abbreviations

IR Infrared

MTL Mass transfer limit

PLIF Planar Laser-induced Fluorescence

SOR Surface Optical Reflectance

UHV Ultra-high Vacuum

2 Introduction

Catalysis has over the last decades become a tool that the manufacturing of chemical products is contingent on. Materials that previously were created via dangerous and lengthy processes now more frequently rely on catalysis in their manufacturing processes. Advancement in catalysis research find new reaction pathways which can reduce the use of dangerous chemicals and make the production more efficient, thus making the development result in economic, environmental, and safety benefits. It can also lead to new possibilities in, for example, medicine development.[1]

Palladium is the catalyst used in this thesis project. One vital area where palladium is used is in the catalytic converter connected to combustion engines. Pd is used to manage by-products that could otherwise be harmful. In combustion engines, the main products are H_2O and CO_2, which are created in complete combustion. There is, however, a contribution of incomplete combustion, which has CO as one of the products. Materials with catalytic properties, such as palladium, are therefore used to manage dangerous by-products, which for CO is to help oxidation of CO into CO_2. CO is a poisonous gas, and efficient oxidation is crucial since many engines are used in populated environments[2]. Although the reaction is common, one main reason to study CO oxidation is that the knowledge of this simple reaction can be applied to more complicated molecules. Improved understanding of the process of splitting the O_2 molecule that occurs to form CO_2 from CO, can be applied to similar reaction such as methanol formation from methane gas, which is an essential reaction in climate applications[3]. Nitric oxides are also a by-product in combustion engines and an important component in environmental research. Since CO and NO oxidation in combination are significant for both environmental applications and industry, synergistic effects can be of interest[4]. CO oxidation in the presence of NO is what this project will focus on.

If a single crystal Pd surface is heated in a CO-O_2 gas-mixture, it will undergo different activity states. At low temperatures, the surface will have a high CO coverage poisoning the surface, but as the temperature gets higher, CO desorption will occur, leaving space at the surface for O_2 molecules to adsorb. Once the surface reaches a critical temperature, the catalyst will quickly reach a high-activity state through a self-accelerating ignition, henceforth referred to as light-off. The self-accelerating light-off of the reaction is due to the oxidation being an exothermic reaction. Simultaneously to the light-off, the surface will begin the formation of a surface oxide. The CO oxidation activity reaches a limit where the access to CO at the surface is limited, known as the mass transfer limit (MTL). The activity is hence limited by access to reactants and not kinetically controlled. When the active sample is cooled down, it will have a quick activity decrease similar to the light-off, referred to as light-down[5]. Previous research has shown that the light-off for a Pd sample will occurs at lower temperatures for higher O_2:CO ratios[6].

There is an active debate within the catalysis field regarding the phase where late transition metals, such as Pd, are active. In a study by Gustafson et al.[5], single or multi-layer oxide has been shown to be at least as active as the metallic surface at Pd unless the thickness reaches bulk oxide dimentions. Others have found that the surface oxide is connected to limitations of the activity[7]. This disagreement is of importance to this thesis since the theoretical research by Lorentzi et al.[8], which will be used as a basis for the project, is done with the assumption that the oxidized surface is inactive. The oxide covered surface is assumed to be oxygen poisoned and thought to be inactive while some part of the surface can be metallic even at high oxygen conditions and therefore

have some activity[8].

Conditions, where experiments have been performed, are often far from realistic with small, simple surfaces, ultra-high vacuum (UHV), and simplified gas conditions. Conclusions about the surface construction and properties from these conditions can often give more understanding of large-scale systems; however, when more complex systems approach realistic conditions, the applications become greater. *In-situ* studies of both reactions and surface structure for both CO and NO oxidation are common. However, studies of the synergistic effects of more complex gas compositions are rare but would have closer connection to real applications. Lorenzi et al. studied simultaneous CO and NO oxidation via a *first-principles kinetic Monte Carlo model*[8]. The prediction from their simulations were that the oxygen coverage of the surface was reduced below the limit where oxide is formed, already at very small partial pressures of NO. Since the criteria used were that an oxidized surface has low activity, referred to as oxygen poisoned, the NO would have a positive effect on the activity under high oxygen conditions. The improved activity stems both from removing oxygen coverage from the surface, and therefore the poisoning, but also other synergistic effects. Even though the NO and CO oxidation might be thought to be competing reactions, the study predicted that the CO oxidation activity would be improved under otherwise inactive states. The CO and NO is in the study assumed to compete for the same surface sites and adsorbed oxygen. The oxidation activity was found to peak at NO partial pressures where the NO effectively prevents the oxide build-up, but before the NO surface coverage is too great and prevents surface access for the CO[8]. The predictions have, however, not been experimentally tested.

There is thus a scientific gap in experimental testing of the role of NO in CO oxidation and further, disagreement in the role of the surface oxide. To experimentally test the predictions by Lorentzi et al.[8], this thesis studies the activity and surface oxidation level with and without the presence of NO. The paper by Lorentzi et al. focuses on high-pressure conditions[8], which are harder to mimic experimentally due to safety hazards of high pressures. The conditions used are therefore chosen to resemble conditions from the paper where NO is concluded to remove oxide and improve the activity, both at higher and lower oxygen partial pressure.

Combining techniques provides a multifaceted method of measuring both gas and surface development when changing the properties to which the sample is exposed. Planar laser-induced fluorescence (PLIF) (see 2.1.1) is used to study the gas diffusion close to the surface, and surface optical reflectance (SOR) (see 2.1.2) measures the reflectivity of the surface to determine to which extent the surface is oxidized and thus has less reflectively. Using these methods at the different gas compositions can show: 1) if NO prevents formation of surface oxide and 2) what effects the NO has on the CO oxidation activity.

The goal is to experimentally test the predictions by Lorentzi et al. and thus observe how the surface reflectively and CO oxidation activity changes when NO is added to CO oxidation catalysis at a single crystal Pd(100) surface[8]. The aim is to conclude the effects of the NO oxidation in the system and, further, examine the role of the surface oxide. The project does not include methods that can determine the surface structure or type of oxidation in great detail or measure the molecules adsorbed at the surface.

2.1 Experimental tools

2.1.1 Planar Laser-induced Fluorescence (PLIF)

The knowledge of surface reactions is greatest at ultra-high vacuum (UHV) when the changes in gas composition above the surface often are neglected. When moving towards realistic gas conditions, the gas composition will change a lot throughout the reaction process and affect the gas-surface interaction. Planar laser-induced fluorescence (PLIF) will be used for *in-situ* imaging of the gas composition by the surface. PLIF operates though a laser, often pulsed to achieve high peak power, that is shaped into a laser sheet. When tuned to a wavelength corresponding to a transition of a medium placed in the sheet, the medium will fluores. The fluorescence can then be measured using a camera, giving a two-dimensionally resolved image of the gas-composition above the surface.[4]

The benefit of PLIF compared to other techniques used in catalysis measurements are the spatial and temporal resolution[4, 9]. PLIF will in this thesis be used to measure the following molecules at the corresponding wavelengths: CO at 230.1 nm, CO_2 at 2.7 μm, and NO at 226 nm. Excitation spectrums and scematic energy diagrams for the transitions can be seen in Figure 1 and Figure 2.

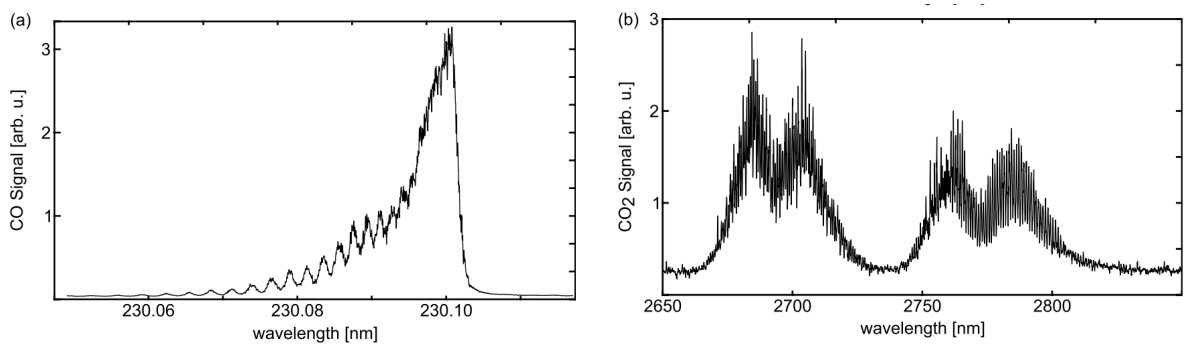

Figure 1: Excitation spectrum at room temperature and 150 mbar for (a) CO and (b) CO_2. Figure source: Zhou et al.[4].

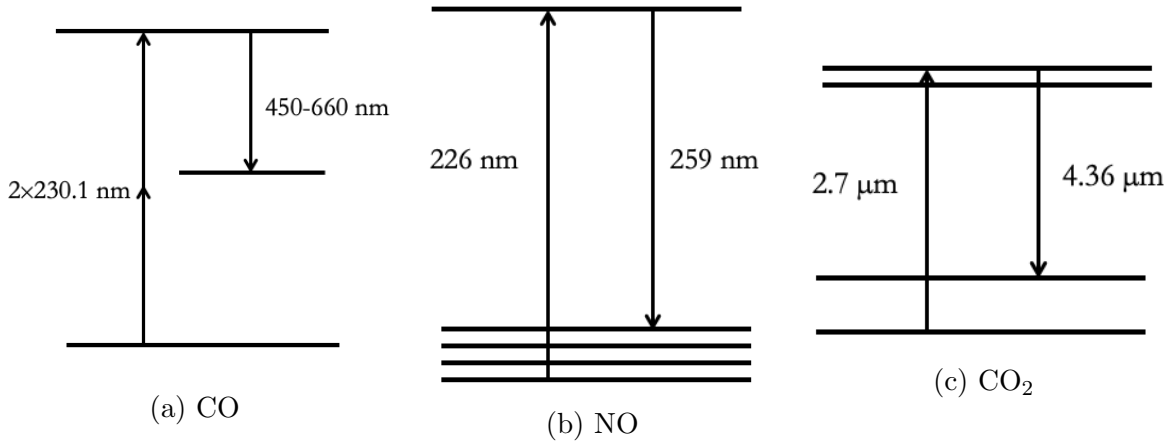

Figure 2: Schematic energy level diagrams for the used transitions in (a) CO PLIF, (b) NO PLIF, and (c) CO_2 PLIF with wavelength used for excitation and the fluorescence wavelength [10, 11].

2.1.2 Surface Optical Reflectance (SOR)

Surface Optical Reflectance (SOR) is a method where the reflectance of collimated LED light of a surface or part of a surface is measured. A schematic image is shown in Figure 3. The reflectance will depend on the surface roughness and the level of oxidation. The Pd atoms will start to difuse during the CO oxidation reactions. The increasing surface oxide during the reaction will lead to a roughening of the surface as a result of a Mars-van Krevelen-type reaction mechanism. The rougher or oxidized surface decreases the specular reflectance and increase the diffuse reflectance which will give less light reflected back to the camera[12, 13]. Without further methods that can distinguish surface structures, it is not possible to determine if a decrease in the SOR signal is due to oxidation or other surface changes that lead to a decreased reflectively. Combining SOR with PLIF allows simultaneous measurements of the gas phase and surface[14]. SOR can be used to show changes over the whole surface, but in this thesis, a region of interest is used to get a mean reflectance throughout a reaction process.

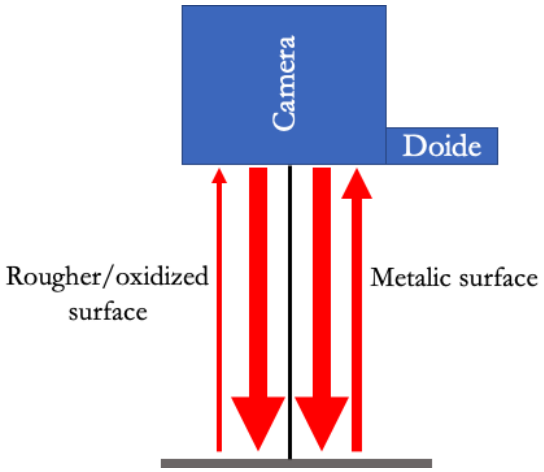

Figure 3: Scematic image if a SOR set-up. The rougher surface will have less specular reflectance and thus lower the signal eaching the camera.

3 Method

3.1 Experimental set-up

3.1.1 Sample

The sample used in this project was a single crystal Pd(100) surface with an 8 mm diameter and 2 mm thickness. The surface was annealed to ensure a smooth single crystal surface and sputtered to remove impurities.

3.1.2 Gas system and Reactor

The sample was placed on a cross-shaped boralectric heater. To measure the temperature, a type D thermocouple, attached to one of the screws of the heating element, was used. The temperature measurements were calibrated to correspond to the temperature of the surface of the sample. The chamber around the sample, henceforth referred to as the reactor, had UV fused silica windows used for SOR, CO PLIF, and NO PLIF. Calcium

fluoride windows were used for the CO_2 PLIF. Different windows were used since they transmit different wavelengths.

The reactor pressure was taken as the average pressure measured at the inflow and outflow to the reactor. For further details on heating and pressure set-up, see the paper by Pfaff et al.[15]. The gases were each controlled by individual mass flow controllers. The gas system was also connected to a mass spectrometer to provide data on the global gas composition in the reactor.

3.1.3 Laser system and SOR

The set-up for the SOR can be seen in Figure 4b. The SOR system consisted of a red 650 nm LED (Thorlabs M625L3) emitting light aimed at the sample through the top window of the reactor. The reflected light was then measured using an Andor Zyla CMOS camera with a Navitar 12x zoom lens.

An image of the optical set-up for CO and CO_2 PLIF can be seen in figure 4a. For the CO PLIF, an injection seeded Nd:YAG laser (Continuum, Powerlite DLS 8010) operating at 532 nm (800 mJ, 10 Hz), second harmonic, was used to pump an R610 dye laser (Continuum, Vista) with ethanol solvent. The dye laser produced an approximately 587.2 nm, 150 mJ output beam. The dye output was frequency-doubled through a BBO crystal (Continuum, Vista FX) to achieve a 293.6 nm, 30 mJ/pulse UV beam, which was then mixed with the 1064 nm residual beam in a second BBO crystal (Continuum, Vista FX), giving a 230.1 nm beam. The beam was directed using a series of UV-fused silica prisms. The reflected beam from one prism was measured by a power meter (Gentec-EO, Maestro) to monitor pulse-to-pulse energy deviations. Before entering the reactor though one of the silica windows, the beam was shaped using a series of lenses to a $\sim$6 mm laser sheet. The sheet was directed to pass the reactor as close to the surface as possible without causing any reflections. The CO fluorescence was measured using an ICCD camera with a B. Halle f=150 mm objective. Images were gathered at a 10 Hz repetition rate corresponding to the laser pulse rate. A specially made interference filter for CO PLIF was used before the camera. It was made to transmit the wavelengths of the CO fluorescence, which is 450-660 nm. The transmission curve of the filter can be seen in Figure 5.

The same set-up as for CO PLIF was used for NO PLIF. To achieve NO fluorescence, the mixer was set to provide a wavelength of 226 nm. No filter was used for the NO PLIF.

For CO_2 PLIF, the 1064 nm beam was used to pump an IR-OPO (GWU, versaScan-L 1064). This generated a 1.7 μm signal beam and a 2.7 μm idler beam. A dichroic mirror was used to separate the two beams. The idler beam was shaped into a $\sim$ 6 mm laser sheet before passing over the surface through the calcium fluoride windows. The fluorescence was measured using an IR camera (Santa Barbara Focal Plane, SBF LP134) cooled with liquid nitrogen. A band-pass filter centered around 4.26 μm, the CO_2 signal wavelength, and a 100 nm width was used. The camera was set to a 20 Hz repetition rate, with every other image being background. The background was subtracted from the CO_2 PLIF signal images. This was necessary since the CO_2 PLIF images have a high thermal background.

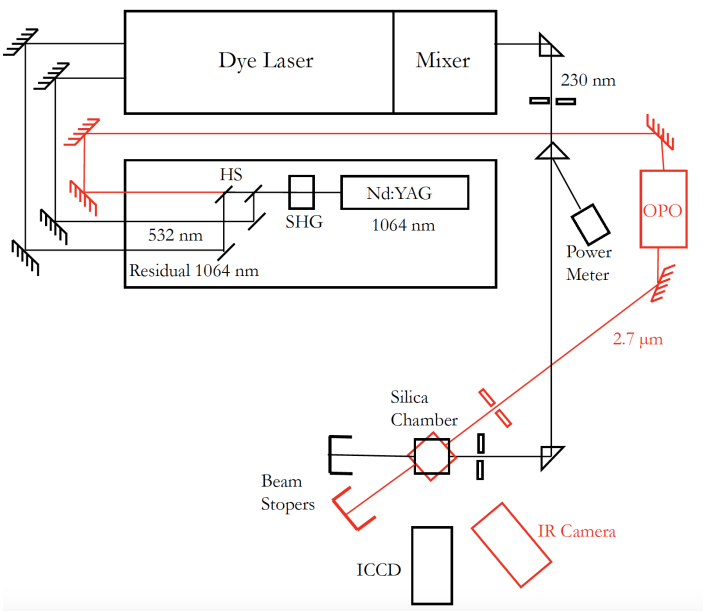

(a) Planar Laser-induced Fluorescence.

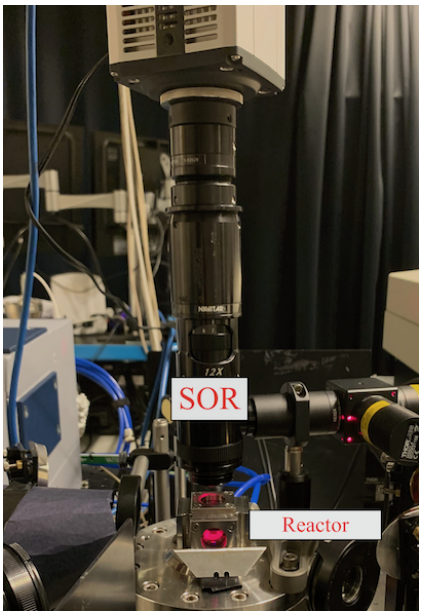

(b) Surface Optical Reflectance

Figure 4: (a) Schematic optical set-up CO PLIF (black) and CO_2 (red). SHG: Second harmonic generator. HS: Harmonics separator. (b) Picture of SOR set-up with camera and LED light mounted over the reactor.

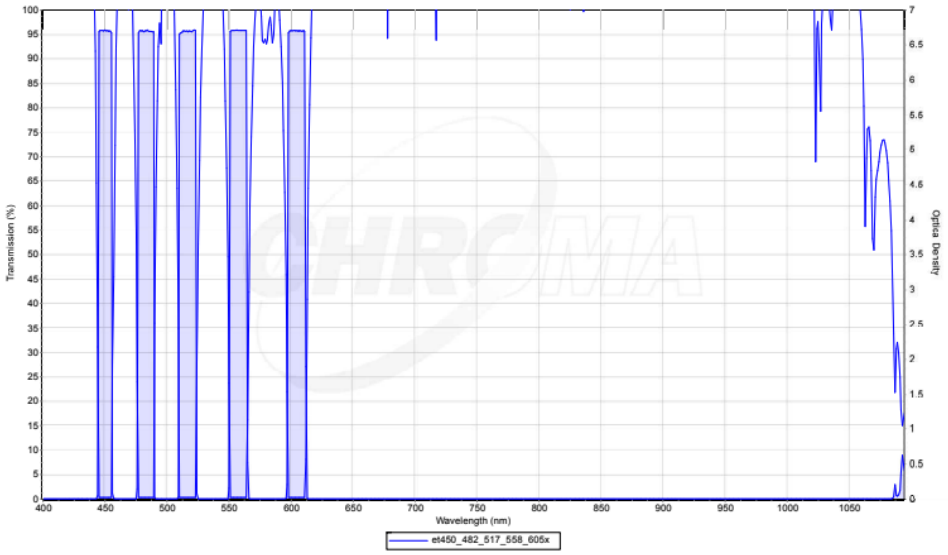

Figure 5: Transmissioin scheme for the special filter for CO PLIF. Transmission (%) on left axis and optical density on the right axis. Figure source: Semrock.

3.2 Measurements

Measurements were performed at four gas conditions with the same total pressure and gas flow per minute (see Table 1). The reactor pressure was ∼265 mbar during the measurements, and a constant flow of 210 ml/min was used. The CO flow was kept constant at 10 ml/min 10 % CO mixed in Ar. Two oxygen environments were used: 10 and 40 ml/min O_2, resulting in 10:1 O_2:CO ratio and 40:1 O_2:CO ratio respectively. Both ratios were tested with 2 ml/min 10 % NO mixed in Ar and without. Ar was used as a buffer gas and changed to keep the constant gas flow.

Table 1: Gas flows (ml/min) used for test ramps. (1) 10:1 O_2:CO ratio (2) 40:1 O_2:CO ratio (3) 10:1 O_2:CO ratio with NO (4) 40:1 O_2:CO ratio with NO. The CO and NO used were 10 % CO/NO mixed with Ar.

	Ar (ml/min)	O_2 (ml/min)	10 % CO (ml/min)	10 % NO (ml/min)
1	190	10	10	0
2	160	40	10	0
3	188	10	10	2
4	158	40	10	2

The reactor was heated to 1.2 A, approximately corresponding to a maximum temperature of 550 K. Ramp-up and ramp-down time was 300 s, and the maximum heating current was constant for 200 s. This heat ramp was used for all measurements and will henceforth be referred to as the test ramp (see Figure 6). The temperature was consistent between measurements and the sample will be assumed to have the same temperature at a given time between different measurements.

After heating the sample, especially at higher O_2 concentrations, bulk oxide could still be noticed at the surface even after the sample had been cooled down. This led to a decrease in reactivity and initial SOR signal. A decrease was further noticeable after reactions involving NO. To restore the initial surface conditions, the surface was heated in only CO and Ar to 2 A, corresponding to approximately 760 K (see Figure 6a).

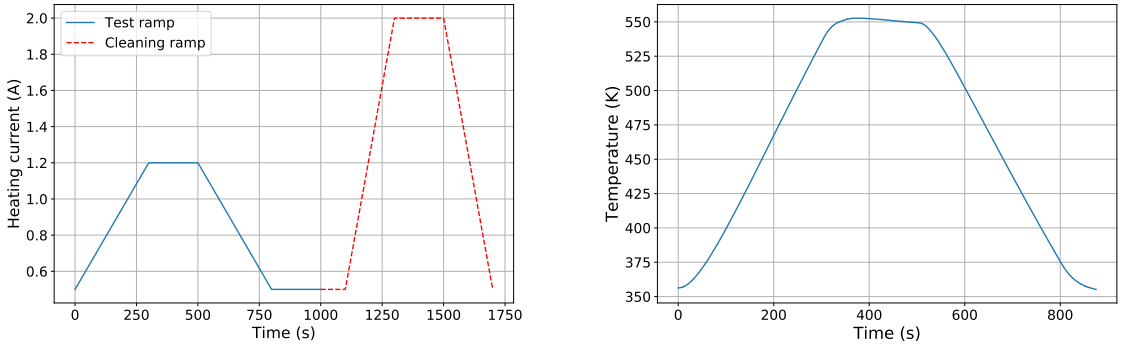

(a) (b)

Figure 6: (a) The current used during the test ramp with the gases described in Table 1 and the cleaning ramp in only CO and Ar. (b) The temperature received by the test ramp in (a).

For all gas compositions, SOR measurements were performed simultaneously as CO or CO_2 PLIF measurements. For compositions including NO, NO PLIF measurements were performed. Additional data on gas flows, reactor temperature, laser power, and mass spectroscopy wes gathered. Most additional data ware only used to control that the conditions were consistent between measurements.

Measurements of the average SOR signal in a region of interest were gathered throughout the test ramp for all gas compositions. Comparisons of the SOR signal intensity at 10:1 O_2:CO ratio and 40:1 O_2:CO ratio can determine the difference in surface oxidation level between the lower and higher oxygen environment. Further, if NO prevents the surface from being oxidized, the SOR signals trends with NO should have a less significant decrease than the same gas ratio without NO. If the surface oxide is fully prevented, then the SOR signal should be constant throughout the reaction process.

The SOR signal intensity is affected by the diluted hotter gas and background changes due to the hotter surface and thus have a decrease in signal for higher temperatures without surface oxidation or other reactions of interest. The SOR signal intensity will also be affected by a shift in focus as the sample is heated, since the SOR set-up has a short depth of focus. A test ramp was performed in only CO and Ar to get a trend of the unoxidized surface for the full ramp. This was then used to normalize the SOR data to get the relative reflected intensity without changes in SOR signal intensity not caused by relevant surface reactions.

Both CO and CO_2 PLIF were used to measure gas composition above the surface. When CO oxidation occurs, the CO fluorescence shown by the CO PLIF signal should decrease and instead show up as CO_2 PLIF signal, which should be close to zero before and after the test ramp. The full fluorescence image can be used to see the full reaction process and where at the surface the reaction takes place. However, to see the change over time, a region of interest was chosen above the surface, of which the average was plotted over time.

Comparing 10:1 O_2:CO ratio CO or CO_2 PLIF signal trends to 40:1 O_2:CO ratio CO or CO_2 PLIF signal trends can show different effects that the higher oxygen environment has on the activity of the catalyst. Further, with comparisons to the SOR signal trends, the effects of different levels of surface oxidation can be observed. The PLIF signal trends for both ratios without NO can then be compared to signal trends from measurements with NO. The comparison between PLIF signal images/trends with and without NO can determine the effects of NO and NO oxidation on the CO oxidation. If the presence of NO prevents the surface oxide, the PLIF images can also give some clarity in the role of the surface oxide.

NO PLIF measurements were performed for test ramps with 10:1 O_2:CO ratio with NO and 40:1 O_2:CO ratio with NO. The NO PLIF signal trend can show the difference in NO oxidation and adsorption activity between the two oxygen environments and provide information regarding the gas conditions effect on NO oxidation.

Since some heat-dependent gas changes will occur regardless of reaction and to compensate for any inconsistencies in the laser sheet, the PLIF images were divided with profile images. The profiles were either received by doing a ramp without O_2, thus without oxidation, or by taking images at high and low temperatures without oxygen and extrapolating in between. To manage background noise, such as reflections from the laser, in the CO and NO PLIF measurements, background images were subtracted from both profiles and results. The PLIF signal is assumed to be linear to the gas concentration by the surface.

4 Results and Discussion

The SOR signal over time for all gas conditions can be seen in Figure 8. The SOR trends for 10:1 O_2:CO ratio without NO and 40:1 O_2:CO ratio without NO show that the reflectance clearly decreases at higher temperatures, indicating the build-up of surface oxide. It can be observed from the SOR measurements for the 10:1 O_2:CO ratio that there is an onset of surface oxide formation at a temperature (447 K) corresponding to light-off of the corresponding CO_2 PLIF signal trend in Figure 8a. This shows that the surface oxide formation is connected to the ignition of the catalyst activity, as described in the introduction. The oxide removal is slightly delayed after the light-down shown in the CO_2 PLIF trend at 402 K. An onset in surface oxide formation of the same order of magnitude as that in the SOR signal for 10:1 O_2:CO ratio can be seen for 40:1 O_2:CO ratio without NO in Figure 7. The oxide formation is initiated before the light-off for 40:1 O_2:CO ratio as can be seen in Figure 8b. The SOR trend can be seen to increase above 1 for 40:1 O_2:CO ratio in Figure 7 which indicates some irregularities since the normalized trend should be ≤ 1.

The SOR signal for 40:1 O_2:CO ratio without NO in Figure 8b shows an accelerated oxide formation at temperatures after the light-off. This higher surface oxide formation is an expected result of the higher oxygen coverage. The surface oxide at 40:1 O_2:CO ratio to the most part remains at the surface when the temperature is lowered, and the effect of the CO oxidation activity light-down is not as significant as for 10:1 O_2:CO ratio.

The SOR signal for both 10:1 O_2:CO ratio with NO and 40:1 O_2:CO ratio with NO can be seen in Figure 8. It can be observed that the signal is approximately unchanged compared to the profile during the full test ramp. That the reflectively is kept constant indicates that the NO prevents the surface oxide formation, as predicted by Lorenzi et al.[8].

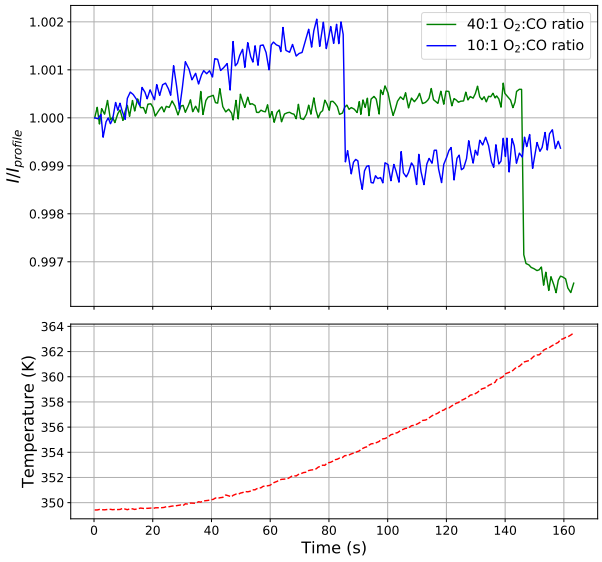

Figure 7: SOR signal trend for 10:1 O_2:CO ratio without NO and 40:1 O_2:CO ratio without NO for a short time-interval within the full test ramp. The SOR signal for the the full test ramp can be seen in Figure 8. The onset of surface oxide formaiton for the 40:1 O_2:CO ratio occurs at 354 K and at 361 K for 10:1 O_2:CO ratio.

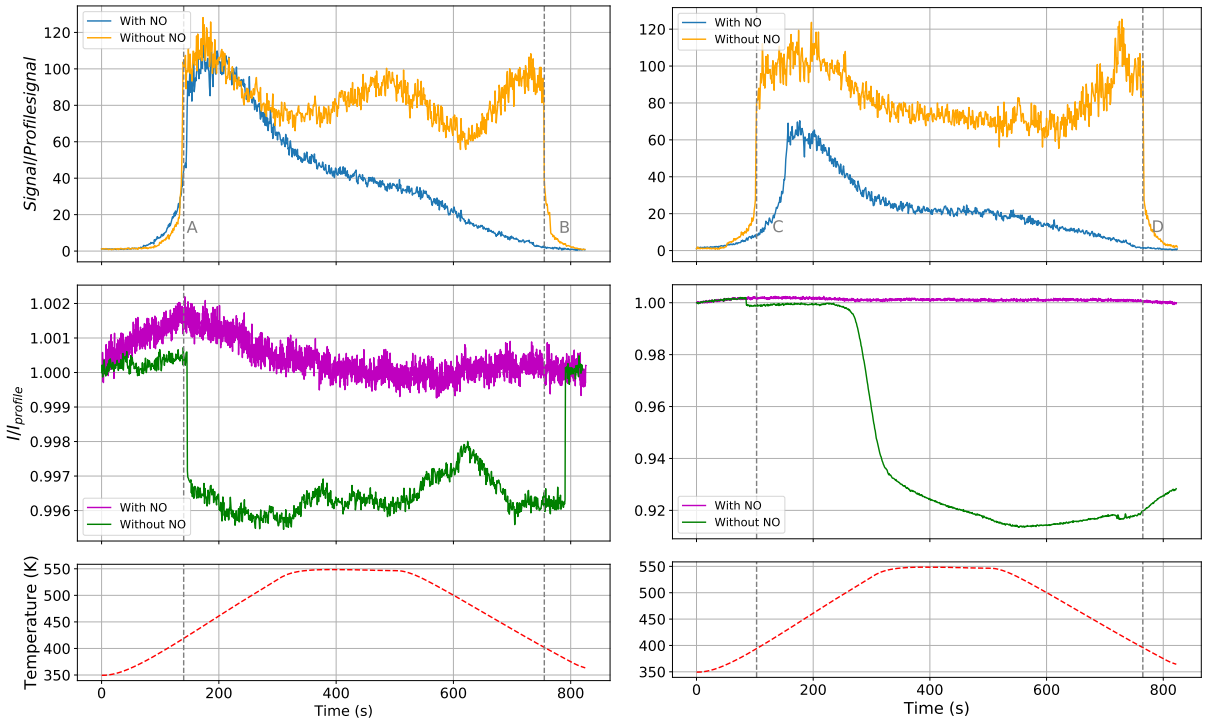

(a) 10:1 O_2:CO ratio.

(b) 40:1 O_2:CO ratio.

Figure 8: CO_2 PLIF signal trend for a region of interest (top) and SOR signal (middle) during the heating ramp (bottom) with 2 ml/min NO and without. The region of interest used for CO_2 PLIF trend can be seen in Figure 9. The SOR signal trends for both ratios with NO is constant. (A) the light-off for 10:1 O_2:CO ratio shown in the CO_2 PLIF trend at 447 K. The SOR trend shows that the oxide build-up onset at the same temperature. The CO_2 PLIF trend for 10:1 O_2:CO ratio with NO follows the same light-off but is then deceased at a higher temperature. (B) the light-down for 10:1 O_2:CO ratio shown in the CO_2 PLIF trend at 402 K. The SOR trend shows that the surface oxide is disappearing at a lower temperature. (C) The light-off for 40:1 O_2:CO ratio shown in the CO_2 PLIF trend at 394 K. The SOR trend shows that the oxide build-up onset at a lower temperature. There is a greater oxide build-up at a higher temperature. The 40:1 O_2:CO ratio with NO has a weaker light-off and is then decreased. (D) the light-down for 40:1 O_2:CO ratio shown in the CO_2 PLIF trend at 396 K. The SOR trend shows that the surface oxide does not have a clear reaction to the light-down and that it is not fully removed.

The CO_2 PLIF signal trend images for 10:1 O_2:CO ratio without NO and 40:1 O_2:CO ratio without NO can be seen in Figure 8. The two trends without NO show that the activity of the catalyst has clear light-offs, light-downs, and MTLs. The activity reached at MTL after the light-off is almost equal between 10:1 O_2:CO ratio and 40:1 O_2:CO ratio. The similarity activity indicates that the MTL truly is caused by a limitation in access to CO at the surface. It can be observed that the light-off occurs at lower temperatures for 40:1 O_2:CO ratio than for 10:1 O_2:CO ratio, which is consistent with the conclusion for higher oxygen environments as described by McClure et al.[16].

The CO_2 PLIF signal trend for 40:1 O_2:CO ratio has a more significant decrease as the sample reaches the maximum temperature (after 200 s in Figure 8b), which can be an effect of bulk oxide formation. Both the earlier light-off and decrease can also be seen in Figure 9a and 9b. The 10:1 O_2:CO ratio images show that the sample is not active at

412 K when the images for 40:1 O_2:CO ratio shows a high activity. The activity for 40:1 O_2:CO ratio is lower at 546 K temperature.

The CO_2 PLIF signal trend in Figure 8a shows that there are similar light-off and activity at MTL for 10:1 O_2:CO ratio with and without NO. This can also be observed in Figure 9a and 9c, where the two first images are similar. There is then a gradual decrease from the activity at MTL at high temperatures. At 546 K, the 10:1 O_2:CO ratio without NO in Figure 9a (III) still shows a high activity while the 10:1 O_2:CO ratio with NO in Figure 9c (IV) is significantly decreased compared to the lower temperature images. The decrease in CO_2 PLIF signal in for 10:1 O_2:CO ratio with NO in Figure 8a is then accelerated as the temperature decrease. The signal shows a small light-down in activity at a higher temperature than without NO.

The CO_2 PLIF signal for 40:1 O_2:CO ratio with NO is further limited as can be seen in Figure 8b and Figure 9d. The trend shows a shape that is similar to that of the 10:1 O_2:CO ratio with NO trend, but with lower maximum activity. The light-off is no longer at a lower temperatures than for 10:1 O_2:CO ratio as for the 40:1 O_2:CO ratio without NO. The MTL activity of the 40:1 O_2:CO ratio without NO is not reached for 40:1 O_2:CO ratio with NO. The light-down can be observed at a higher temperature than for the same ratio with NO.

The CO_2 PLIF signal trend in Figure 8 show that the presence of NO limits the CO oxidation. The limitation is more significant at 40:1 O_2:CO ratio than at 10:1 O_2:CO ratio. The 10:1 O_2:CO ratio with NO is first affected by the NO presence after the light-off while the 40:1 O_2:CO ratio with NO has a limited light-off that does not reach the MTL.

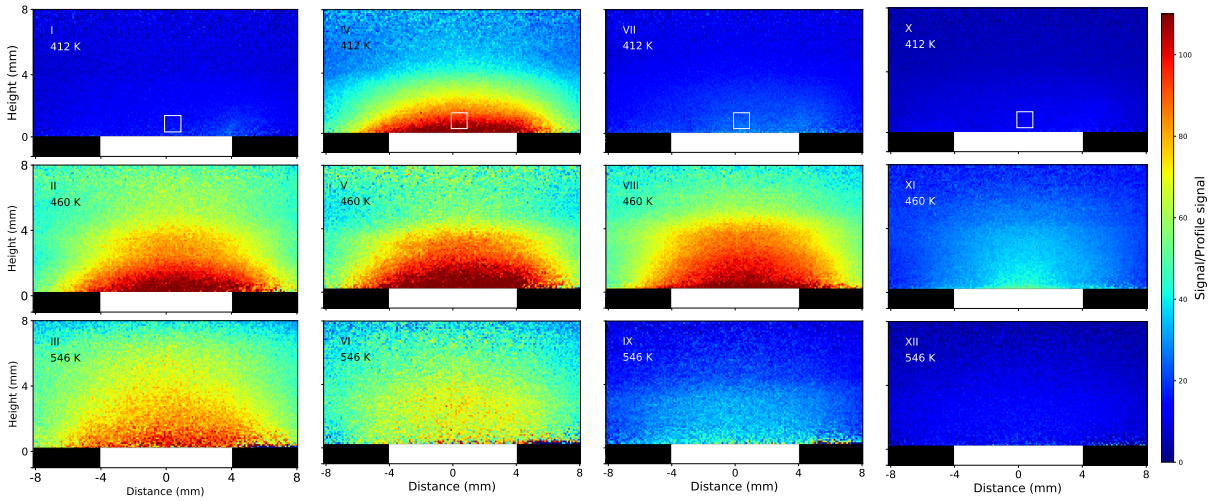

(a) O_2:CO ratio 10:1 Without NO

(b) O_2:CO ratio 40:1 Without NO

(c) O_2:CO ratio 10:1 With NO

(d) O_2:CO ratio 40:1 With NO

Figure 9: CO_2 PLIF images at 412, 460, and 546 K. The large white area marks the area where the sample is. The small square is the region of interest for Figure 8. Comparing (I) and (IV) shows that 40:1 O_2:CO ratio has CO oxidation activity at a lower temperature than 10:1 O_2:CO ratio. (I-II) is similar to (VII-VIII) which indicates that the activity for 10:1 O_2:CO ratio with NO initially behaves as 10:1 O_2:CO ratio without NO, but the difference between (III) and (IX) show that the activity is limited at higher temperatures with NO. (d) compared to (b) show that the activity is completely limited for 40:1 O_2:CO ratio with NO, especially at higher temperatures.

The increase in CO_2 PLIF signal in Figure 8 has a corresponding decrease in CO PLIF signal for all conditions, which can be seen in Figure 10. The decrease at higher temperatures at 40:1 O_2:CO ratio without NO in Figure 8b can also be observed in Figure 10b. The ratio of minimum CO PLIF signal between 40:1 O_2:CO ratio with and without NO in Figure 10b is similar to that in maximum CO_2 PLIF signal in Figure 8b. However, the earlier light-off for 40:1 O_2:CO ratio seen in Figure 8b is not visible in Figure 10b. Laser reflections caused overexposure in the time interval $t = 153-175$ s in the 40:1 O_2:CO ratio without NO CO PLIF trend. It has been assumed to have the same intensity as at $t = 152$ s.

CO PLIF images for both ratios with and without NO at three different temperatures can be seen in Figure 11. The decrease in CO PLIF signal can be seen to mirror the increase in CO_2 PLIF signal in Figure 9. Reflections on the right edge of the sample can be observed, especially in the images for 40:1 O_2:CO ratio without NO. The unstable signal for the CO PLIF at 40:1 O_2:CO ratio might be part of the cause of the absences of the earlier light-off. The CO PLIF trend for 40:1 O_2:CO ratio with NO had some noise due to laser reflections, which were removed.

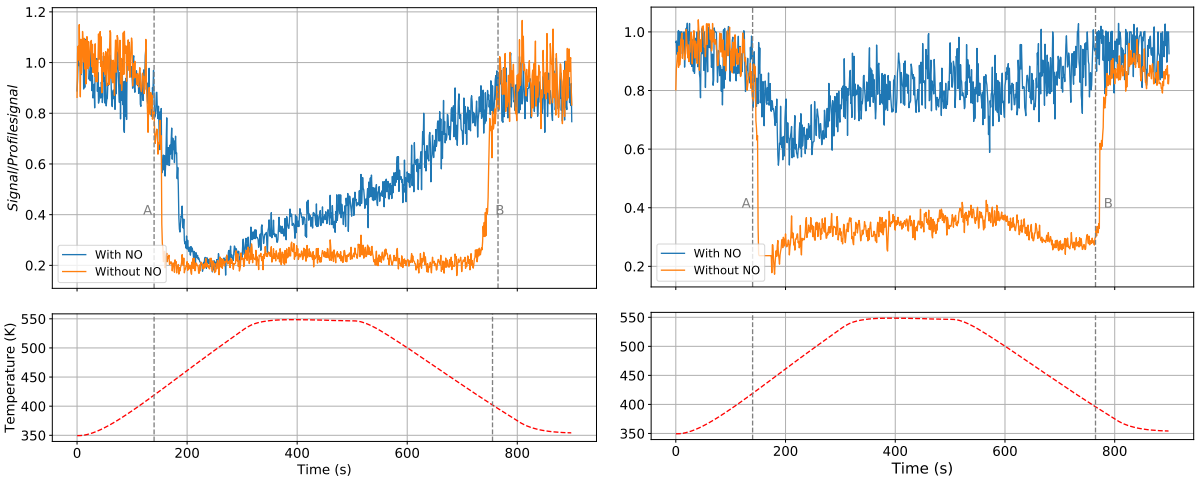

(a) 10:1 O_2:CO ratio

(b) 40:1 O_2:CO ratio

Figure 10: CO PLIF trend (top) during the heating ramp (bottom) with 2 ml/min 10 % NO and without. (A) and (B) are the lines in Figure 8a. The CO PLIF trend for 40:1 O_2:CO ratio does not show a light-off at a lower temperature as seen in Figure 8b. The light-off and light-down for 10:1 O_2:CO ratio occur at similar temperatures as seen in the CO_2 PLIF trend. There is a clear decrease between the light-off and light-down for 40:1 O_2:CO ratio.

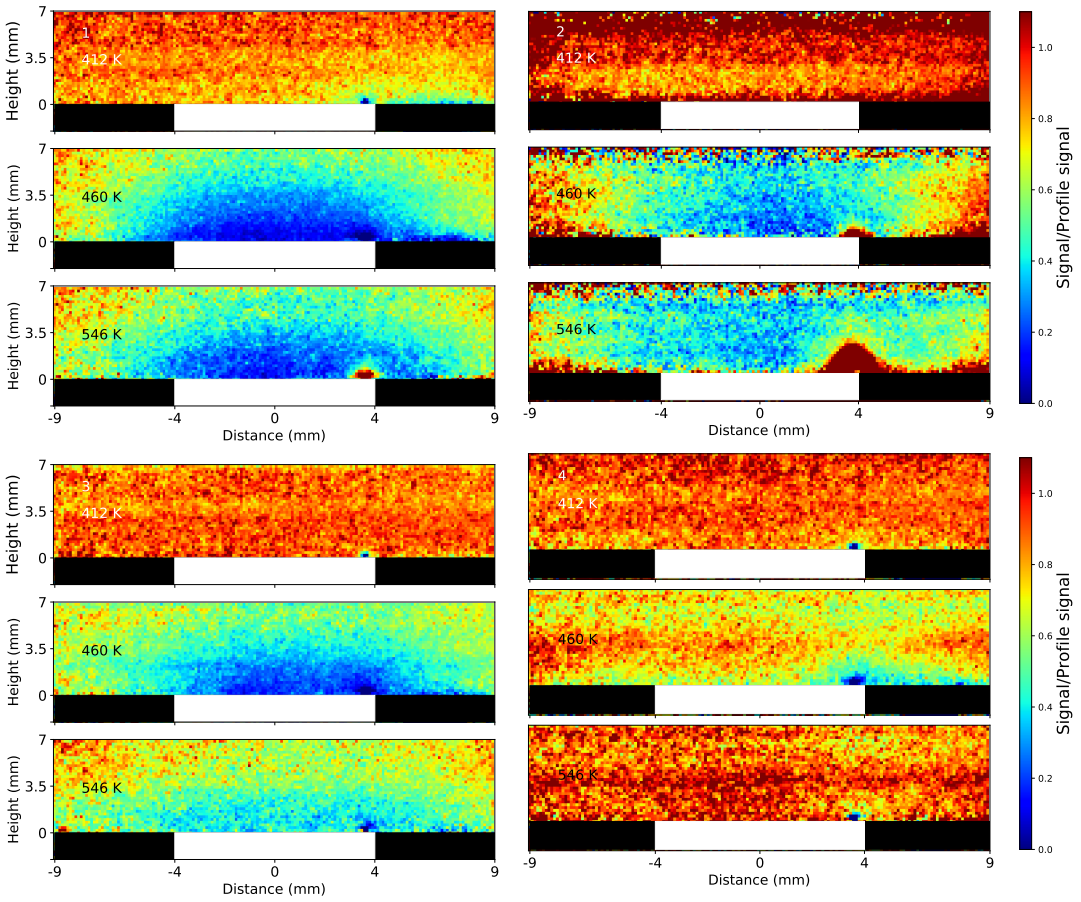

(a) O_2:CO ratio 10:1

(b) O_2:CO ratio 40:1

Figure 11: CO PLIF images for 10:1 O_2:CO ratio and 40:1 O_2:CO ratio at three different temperatures without NO (1-2) and with NO (3-4). The images can be seen to mirror those for CO_2 PLIF in Figure 9.

In the NO PLIF signal trend for 10:1 O_2:CO ratio with NO and 40:1 O_2:CO ratio with NO in Figure 12, a decrease in NO signal at higher temperatures can be observed, which can indicate the creation of NO_2. The decrease can also imply NO adsorption at the surface. The decrease in signal has no clear ignitions but shows a quite clear temperature dependence for both ratios. The NO signal was not as strong as the CO and CO_2 PLIF signals, and the effects of background reflections were more noticeable. The NO PLIF trend have had some reflections removed.

NO PLIF images for 40:1 O_2:CO ratio with NO at the lowest and highest temperature of the test ramp can be seen in Figure 13. The decrease is quite even over the laser sheet but with a small gradient over the sample at higher temperature.

If the previously discussed decrease in CO oxidation activity when NO is added were due to the NO oxidation being a reaction competing for reactants, the reaction would be oxygen-limited and thus be more limited at 10:1 O_2:CO ratio. The result in Figure 12 shows that the NO PLIF signal for 40:1 O_2:CO ratio shows less NO oxidation, which contradicts this as an explanation. Both the CO oxidation and NO oxidation are more restricted at 40:1 O_2:CO ratio with NO than 10:1 O_2:CO ratio with NO.

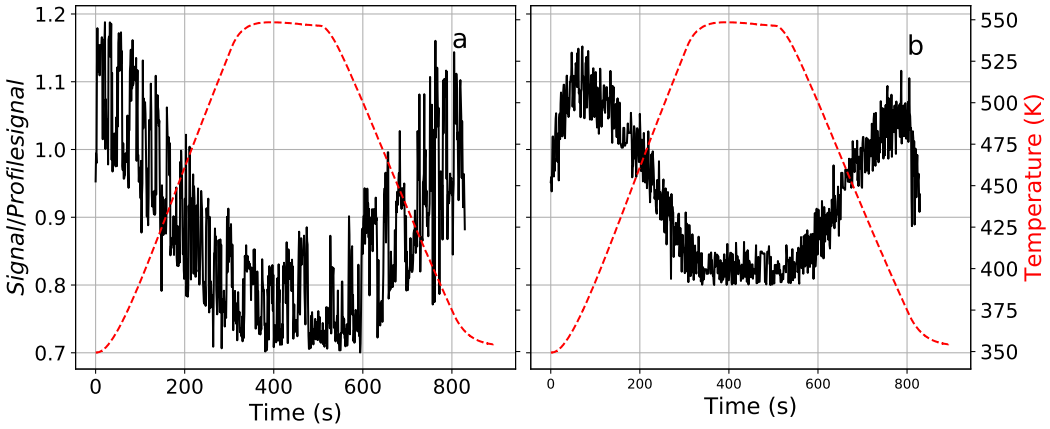

Figure 12: NO PLIF trend at a) 10:1 O_2:CO ratio and b) 40:1 O_2:CO ratio and temperature ramp (red). Both ratios show a decrease at higher temperature but no light-off or light-down. The 10:1 O_2:CO ratio has a greater decrease than the 40:1 O_2:CO ratio.

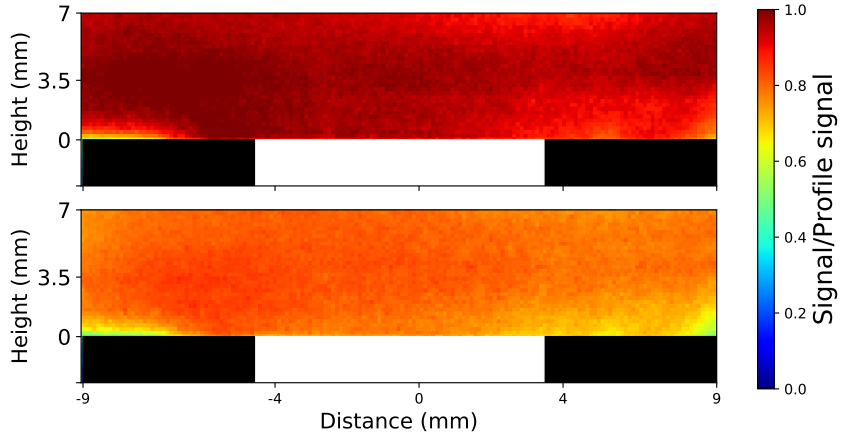

Figure 13: NO PLIF image at 360 K (top) and 550 K (bottom) for 40:1 O_2:CO ratio with NO. The decrease is quite even throughout the laser sheet but with a slight gradient just above the sample.

The SOR signal trend in Figure 8 clearly shows that the NO presence prevents the build-up of surface oxide. This observation is in agreement with the prediction by Lorentzi et al.[8]. However, on the contrary to the predictions from the theoretical study, the PLIF signal images and trends show that there is no increase in CO oxidation activity in the presence of NO. Both the CO and CO_2 PLIF signal trend in Figure 8 and Figure 10, and PLIF signal images in Figure 9 show that adding NO to the gas-mixture limits the CO oxidation. This effect has a presence after the light-off for 10:1 O_2:CO ratio. For the 40:1 O_2:CO ratio, the NO limits the light-off both in when it occurs and from reaching MTL. The limitation can not be caused by competition between CO and NO oxidation in access to oxygen since this would limit the 10:1 O_2:CO ratio more than the 40:1 O_2:CO. There is a smaller decrease in NO PLIF signal at 40:1 O_2:CO ratio, which would entail that the NO oxidation also is limited at these conditions.

The decrease in CO oxidation activity at the presence of NO can indicate the importance of the surface oxide to the active state of Pd(100). If the metallic surface does not have a greater activity than the surface with a thin surface oxide, the main consequence of the addition of NO would be NO coverage of the surface, preventing the access for CO.

This contradicts parts of the theoretical basis, were the oxidation activity was found to peak at NO partial pressures where the NO effectively prevents the oxide build-up, but before the NO surface coverage is too great and prevents surface access for the CO. As described by Lorentzi et al.[8], NO and CO can compete for the same surface sites. If the removal does not have positive effects, NO will be preventing reactants from interacting at the sample surface. The NO appears to stick to the surface and disturbs the reaction even when the temperature is low. However, detailed understanding of the behavior at the surface would require additional tools for measurements, such as PM IRRAS.

5 Conclusions

Measurements with SOR and CO, CO_2, and NO PLIF were performed at a single crystal Pd(100) surface with 10:1 O_2:CO ratio and 40:1 O_2:CO ratio both with and without NO. The behavior of the CO oxidation without NO is in good agreement with previous research. The result of the SOR measurements showed that NO prevented surface oxide formation at 10 % NO 2 ml/min in a total gas flow of 210 ml/min, even at higher oxygen conditions where the oxide build-up would otherwise be high. However, the CO oxidation activity was limited by the presence of NO, especially at 40:1 O_2:CO ratio. The limitation can be determined not to be caused by CO and NO competing for oxygen since it can be observed in NO PLIF trends that the NO oxidation activity is higher at 10:1 O_2:CO ratio than 40:1 O_2:CO ratio. The lower CO oxidation activity is thus concluded to be due to NO adsorbed at the surface limits the surface access for the CO.

6 Outlook

Due to the strong ties to the theoretical work by Lorentzi et al. [8], further work could again be connected through looking further at the used conditions. Similar measurements as in this thesis but with more gas-conditions could be performed, which could further find limits where NO has different effects on the activity and find gas composition limits where the different effects occur. These tests could also focus more on NO PLIF to further conclude how the NO oxidation is affected by different gas compositions.

Furthermore, it would also be of interest to connect the studies to more surface detailed research. If the surface structure and gas adsorption could be further determined, the source of the CO and NO oxidation limitations could be determined. For example, use High Energy Surface X-Ray Diffraction to get information on the oxide formation throughout the process and more detailed information about the behavior of the NO at the surface. The knowledge of the surface oxide and surface structure could also be improved using PM IRRAS or AP-XPS to get surface information.

References

[1] H. K. Newhall. Kinetics of engine-generated nitrogen oxides and carbon monoxide. In *Symposium (International) on Combustion*, volume 12, pages 603–613. Elsevier, 1 1969.

[2] P. Tribolet and L. Kiwi-Minsker. Palladium on carbon nanofibers grown on metallic filters as novel structured catalyst. In *Catalysis Today*, volume 105, pages 337–343. Elsevier, 8 2005.

[3] J. Zetterberg, S. Blomberg, J. Gustafson, J. Evertsson, J. Zhou, E. C. Adams, P. A. Carlsson, M. Aldén, and E. Lundgren. Spatially and temporally resolved gas distributions around heterogeneous catalysts using infrared planar laser-induced fluorescence. *Nature Communications*, 6, 5 2015.

[4] J. Zhou, S. Pfaff, E. Lundgren, and J. Zetterberg. A convenient setup for laser-induced fluorescence imaging of both CO and CO2 during catalytic CO oxidation. *Applied Physics B: Lasers and Optics*, 123(3):87, 3 2017.

[5] J. Gustafson, O. Balmes, C. Zhang, M. Shipilin, A. Schaefer, B. Hagman, L. R. Merte, N. M. Martin, P. A. Carlsson, M. Jankowski, E. J. Crumlin, and E. Lundgren. The Role of Oxides in Catalytic CO Oxidation over Rhodium and Palladium. *ACS Catalysis*, 8(5):4438–4445, 5 2018.

[6] M. S. Chen, Y. Cai, Z. Yan, K. K. Gath, S. Axnanda, and D. Wayne Goodman. Highly active surfaces for CO oxidation on Rh, Pd, and Pt. *Surface Science*, 601(23):5326–5331, 12 2007.

[7] R. van Rijn, O. Balmes, A. Resta, D. Wermeille, R. Westerström, J. Gustafson, R. Felici, E. Lundgren, and J. W. M. Frenken. Surface structure and reactivity of Pd(100) during CO oxidation near ambient pressures. *Physical Chemistry Chemical Physics*, 13(29):13167, 2011.

[8] J. M. Lorenzi, S. Matera, and K. Reuter. Synergistic Inhibition of Oxide Formation in Oxidation Catalysis: A First-Principles Kinetic Monte Carlo Study of NO + CO Oxidation at Pd(100). *ACS Catalysis*, 6(8):5191–5197, 8 2016.

[9] S. Pfaff, J. Zhou, U. Hejral, J. Gustafson, M. Shipilin, S. Albertin, S. Blomberg, O. Gutowski, A. Dippel, E. Lundgren, and J. Zetterberg. Combining high-energy X-ray diffraction with Surface Optical Reflectance and Planar Laser Induced Fluorescence for operando catalyst surface characterization. *Review of Scientific Instruments*, 90(3):033703, 3 2019.

[10] J. Bradshaw and D. D. Davis. Sequential two-photon-laser-induced fluorescence: a new method for detecting atmospheric trace levels of NO. *Optics Letters*, 7(5):224, 5 1982.

[11] J. Gustafson J. Zetterberg S. Blomberg, J. Zhou and E. Lundgren. 2D and 3D imaging of the gas phase close to an operating model catalyst by planar laser induced fluorescence.

[12] W. G. Onderwaater, A. Taranovskyy, G. M. Bremmer, G. C. Van Baarle, J. W.M. Frenken, and I. M.N. Groot. From dull to shiny: A novel setup for reflectance difference analysis under catalytic conditions. *Review of Scientific Instruments*, 88(2):023704, 2 2017.

[13] W. G. Onderwaater, A. Taranovskyy, G. C. Van Baarle, J. W.M. Frenken, and I. M.N. Groot. In Situ Optical Reflectance Difference Observations of CO Oxidation over Pd(100). *Journal of Physical Chemistry C*, 121(21):11407–11415, 6 2017.

[14] Jianfeng Zhou, Sara Blomberg, Johan Gustafson, Edvin Lundgren, and Johan Zetterberg. Simultaneous Imaging of Gas Phase over and Surface Reflectance of a Pd(100) Single Crystal during CO Oxidation. *The Journal of Physical Chemistry C*, 121(42):23511–23519, 10 2017.

[15] S. Pfaff, H. Karlsson, F. A. Nada, E. Lundgren, and J. Zetterberg. Temperature characterization of an operando flow reactor for heterogeneous catalysis. *Journal of Physics D: Applied Physics*, 52(32):324003, 6 2019.

[16] S. M. McClure and D. W. Goodman. New insights into catalytic CO oxidation on Pt-group metals at elevated pressures. *Chemical Physics Letters*, 469(1-3):1–13, 2 2009.